

VLBA SiO maser observations of the OH/IR star OH 44.8-2.3: magnetic field and morphology

N. Amiri¹, W. H. T. Vlemmings², A. J. Kemball³
and H. J. van Langevelde⁴

¹Sterrewacht Leiden, Leiden University, Niels Bohrweg 2, 2333 CA Leiden, The Netherlands

²Chalmers University of Technology, Onsala Space Observatory, SE-439 92, Onsala, Sweden

³Joint Institute for VLBI in Europe (JIVE), Postbus 2, 7990 AA Dwingeloo, The Netherlands

⁴Department of Astronomy and Institute for Advanced Computing Applications and
Technologies/ NCSA, University of Illinois at Urbana-Champaign, 1002 W. Green Street,
Urbana, IL 61801, USA

Abstract. We report on Very Long Baseline Array SiO maser observations of the OH/IR star OH 44.8 - 2.3. The observations show that the maser features form a ring located at a distance of 5.4 AU around the central star. The masers show high fractional linear polarization up to 100%. The polarization vectors are consistent with a dipole field morphology. Additionally, we report a tentative detection of circular polarization of 7% for the brightest maser feature. This indicates a magnetic field of 1.5 ± 0.3 G. The SiO masers and the 1612 MHz OH masers suggest a mildly preferred outflow direction in the circumstellar environment of this star. The observed polarization is consistent with magnetic field structures along the preferred outflow direction. This could indicate the possible role of the magnetic fields in shaping the circumstellar environment of this object.

Keywords. Stars, Magnetic Fields, Maser, Polarization

1. Introduction

SiO maser emission occurs in the inner circumstellar envelopes (CSEs) of asymptotic giant branch (AGB) stars and can be studied at high angular resolution using high resolution radio interferometers. Very long baseline interferometry (VLBI) observations of the masers in Mira variables have shown that the masers are confined to a region, sometimes ring-shaped, between the stellar photosphere and the dust formation zone (e.g. Cotton *et al.* 2008). Furthermore, VLBI observations revealed that the masers are significantly polarized with linear polarization fractions up to 100%. The circular polarization of the masers is in the range 3% to 5% (Kemball *et al.* 2009).

No information is available at high angular resolution for SiO masers in higher mass loss OH/IR stars. These objects have larger CSEs and much longer periods up to 2000 days than do Mira variables (Herman & Habing 1985). They are strong 1612 MHz OH maser emitters (Baud *et al.* 1979). The stars are surrounded by thick dust shells, which makes them optically obscured. Here, we report the SiO maser polarimetric observations of the OH/IR star OH44.8-2.3 with the VLBA. The observations enable us to obtain the spatial distribution of the SiO maser features in OH/IR stars for the first time. Additionally, our experiment probes the magnetic field strength and morphology in the SiO maser region of OH/IR stars and compares them with those of Mira variables.

2. Observations

We observed the $v=1$, $J = 1 \rightarrow 0$ SiO maser emission toward OH 44.8-2.3 on 6 July 2010 using the Very Long Baseline Array (VLBA) at 43 GHz. The observations were performed in dual circular polarization spectral line mode. The DiFX correlator was used with a bandwidth of 4 MHz and 1024 spectral channels, which results in 0.03 km s^{-1} spectral resolution.

Auxiliary Expanded Very Large Array (EVLA) observations were performed to measure the absolute electric vector polarization angle (EVPA) for the polarization calibrators. We observed the continuum sources J2253+1608 and J1751+0939 as transfer calibrators. The observations were performed in continuum mode and full polarization, using two 128 MHz spectral windows.

3. Results

3.1. Total Intensity

Fig. 1 shows the SiO maser emission map of OH 44.8-2.3 obtained from the VLBA observations. The emission is summed over all velocity channels. The maser features form a partial ring of 4.75 mas. The emission exhibits two opposite arcs and appears to be absent from the western and eastern side of the ring. Assuming a distance of 1.13 kpc obtained from the phase lag method (Van Langevelde *et al.* 1990), the ring radius corresponds to 5.4 AU. Feature 1 exhibits the largest flux density of 2.8 Jy. The ring pattern observed for the SiO emission indicates the tangential amplification of the masers.

3.2. Linear Polarization

The polarization morphology of the SiO maser emission is shown in Fig. 1. The Stokes parameters (I, Q, and U) are summed over frequency. The polarized emission is plotted as vectors with a length proportional to the polarization intensity. The position angle of the vectors corresponds to the EVPA of the emission. The background contours show the total intensity. The observations reveal that the SiO maser features of OH 44.8-2.3 are highly linearly polarized with an average linear polarization fraction of 30%. The highest polarization fraction corresponds to 100% for feature 8.

The high fractional linear polarization observed for SiO masers could indicate the anisotropic pumping origin of the masers. It was shown that anisotropic background radiation from the central star generates anisotropic pumping, potentially producing a high degree of linear polarization in the SiO maser region (e.g. Watson 2002). However, the results from Nedoluha & Watson (1990) show that the polarization vectors still trace the direction of the magnetic field despite the possibility that the linear polarization develops from anisotropic pumping.

The observations show that the SiO masers of OH 44.8-2.3 are in a regime that $g\Omega \gg R > \Gamma$; where R , $g\Omega$, and Γ represent the stimulated emission rate, the Zeeman rate, and the collisional and radiative decay rate, respectively. In this regime the linear polarization vectors appear either parallel or perpendicular to the projected magnetic field, depending on the angle between the magnetic field direction and the line of sight (Goldreich *et al.* 1973). When taking the EVPA of -50° for feature 8, which has the highest linear polarization fraction, this implies that the magnetic field direction is either parallel (-50°) or perpendicular (40°) to the linear polarization vectors. In either case, the EVPA vectors probably indicate a large-scale magnetic field in the SiO maser region of this star.

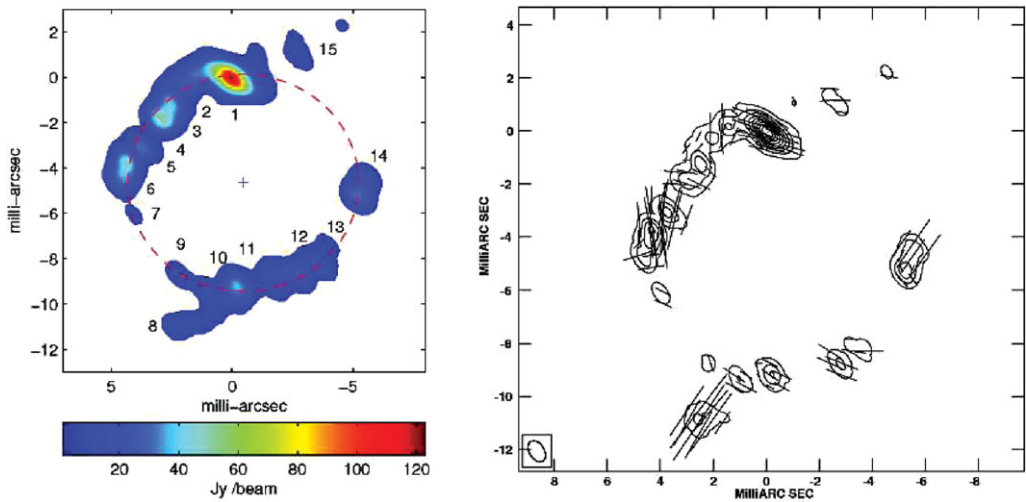


Figure 1. Left Panel: The VLBA map of $v=1, J = 1 \rightarrow 0$ SiO maser emission towards the OH/IR star OH 44.8-2.3. The features are color-coded according to the flux density (Jy / beam) integrated over all velocity channels. Right panel: Contour plot of the Stokes I image at levels [1, 2, 5, 10, 20, 40, 80, 100]% of the peak. Vectors are overlaid proportional to the linearly polarized intensity (on a scale 1 mas = 1.25 Jy beam⁻¹) and drawn at a position angle of the EVPA. All Stokes parameters (I,Q,U) are summed over velocity.

The linear polarization morphology is consistent with the dipole magnetic field morphology in the SiO maser region of this star. However, we cannot rule out toroidal or solar type field morphologies. Polarimetric observations of the OH and H₂O maser regions of the CSE of this star are required to clarify its magnetic field morphology.

3.3. Circular Polarization

We report a tentative detection of 7% for the circular polarization fraction for feature 1 in the modest spectral resolution dataset which has 128 spectral channels (Fig. 1). However, due to the increased noise in the high spectral resolution dataset (1024 spectral channels), we cannot confirm the detection. Further polarimetric VLBI observations of the SiO masers of this star with more integration time are needed to clarify this. The left panel in Fig. 2 shows the total intensity spectrum and the circular polarization profile of feature 1. The V spectrum is plotted after removing a scaled down version of the Stokes I spectrum, which is caused by the instrumental gain differences between the right circular polarization (RCP) and the left circular polarization (LCP) profiles.

We note that, based on polarization studies, we cannot distinguish between the Zeeman and non-Zeeman effects from the observations. Since the SiO masers are in the regime where $g\Omega \gg R > \Gamma$, the non-Zeeman effect introduced by Wiebe & Watson (1998) is applicable. According to this scenario the circular polarization can be generated if the magnetic field orientation changes along the direction of maser propagation. The circular polarization produced from this scenario is on average $\sim \frac{m_l^2}{4}$, where m_l indicates the linear polarization fraction. For the 7% linear polarization fraction measured for feature 1, the generated circular polarization it causes is 0.12%. This implies that the measured circular polarization for feature 1 is about six times higher than the estimated value from the non-Zeeman effect. Wiebe & Watson (1998) show that if the circular polarization is higher than the average of $\frac{m_l^2}{4}$, the circular polarization stems from other causes, probably the Zeeman effect. Therefore, it is likely that the circular polarization of this star comes

from the Zeeman splitting. However, Wiebe & Watson (1998) explain that the average circular polarization in individual features can go up to 20%.

Assuming the Zeeman interpretation of the observed circular polarization, the magnetic field derived from circular polarization corresponds to the following equation (Kemball & Diamond 1997):

$$B = 3.2 \times m_c \times \Delta\nu_D \times \cos\theta, \quad (3.1)$$

where m_c , $\Delta\nu_D$, and θ indicate the fractional circular polarization, the maser line width, and the angle between the magnetic field and line of sight, respectively. The full width half maximum line width for the Stokes I spectrum of feature 1 corresponds to $\sim 0.8 \text{ km s}^{-1}$. Using the preceding relation, a magnetic field of $1.8 \pm 0.5 \text{ G}$ is derived for feature 1.

Alternatively, we use the cross-correlation method introduced by Modjaz *et al.* (2005) to measure the magnetic field due to the Zeeman splitting. In this method the right circular polarization (RCP) and the left circular polarization (LCP) spectra are cross-correlated to determine the velocity splitting. The magnetic field is determined by applying the Zeeman splitting coefficient for SiO masers. We measured a magnetic field of $1.5 \pm 0.3 \text{ G}$ for feature 1.

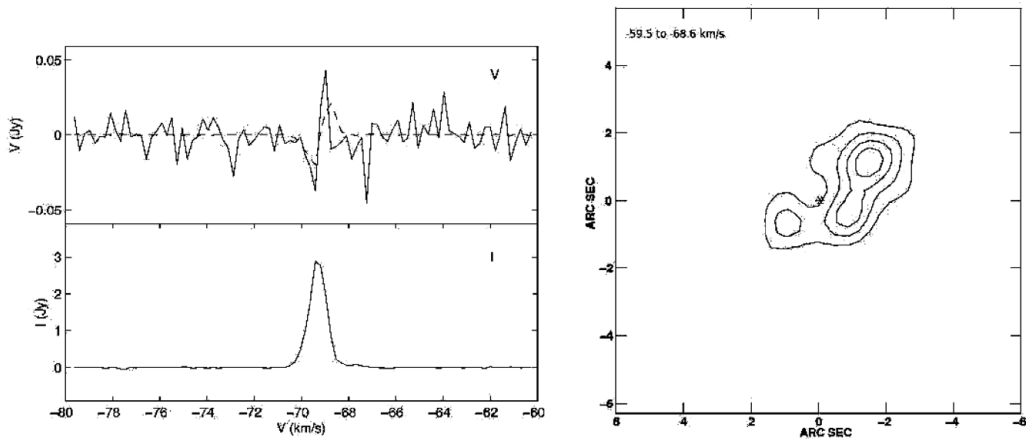


Figure 2. Left panel: Total power (I) and circular polarization (V) spectra of the brightest SiO maser feature of OH 44.8-2.3. The dashed line is the fit to the observed V-spectrum. The V spectrum is shown after removing the scaled down replica of Stokes I. Right panel: 1612 MHz OH maser red-shifted emission map of OH 44.8-2.3 summed over several velocity channels from -59.5 to -68.6 km s^{-1} . The red-shifted peak exhibits the highest flux density of 8.1 Jy . The contour levels are at 0.005 , 0.011 , 0.016 , 0.022 , and 0.027 Jy . The star symbol indicates the position of the peak in the red-shifted emission which probably indicates the position of the central star.

3.4. OH maser observations of OH 44.8-2.3

We found previous observations of the 1612 MHz OH masers of OH 44.8-2.3 using the Very Large Array (VLA) in the NRAO archive. The observations were performed, under project name 'AH127', in the A configuration, which gives a resolution of $1''$. The right panel in Fig. 2 displays a 1612 MHz OH maser map of this star. The emission is summed over several channels slightly red-shifted to the stellar velocity (from -59.5 to -68.6 km s^{-1}).

The 1612 MHz OH masers of this star indicate an elongated shell morphology in the direction where there is a gap in the SiO maser emission (Fig. 1; left panel). We note that

the OH masers occur on much larger scale (~ 1471 AU) than the SiO masers (5.4 AU) around the star. It is therefore not obvious that both deviations from symmetry are related, but if they are, this indicates that there is a mechanism at work that can support the asymmetry on many scales.

Interestingly, the direction of the magnetic field is parallel or perpendicular to the location of the gaps in the SiO maser ring and the OH maser extent. This could indicate that there is a large-scale magnetic field that imposes a preferred direction on the outflow on scales that span two orders of magnitude. Since the timescales involved in forming the OH shell is much larger than that for SiO masers, one would then conclude that the magnetic field is important for imposing an asymmetric signature on the neutral outflow in the OH/IR phase. Furthermore, the high fractional linear polarization measured for the SiO masers of this star could potentially indicate the possible role of the magnetic field in shaping the circumstellar environment of this star.

4. Summary

We performed a pilot study to observe the SiO maser emission in OH/IR stars which have higher mass loss rates compared to Mira variables. Our observations indicate a ring morphology for the SiO maser region of the OH/IR star OH 44.8-2.3. The ring pattern is similar to what was observed previously for Mira variables. The SiO maser features exhibit high fractional linear polarization up to 100%. The polarization vectors are consistent with a dipole field morphology. Additionally, we report a tentative detection of circular polarization at 7% for the brightest maser feature, which corresponds to a magnetic field of 1.5 ± 0.3 G, assuming the Zeeman interpretation for the observed polarization.

In particular, we found that the observed polarization is consistent with magnetic field structures along the preferred outflow direction. This could potentially indicate a role of the magnetic field in shaping the circumstellar environment of this object, and that magnetic fields thus could be important for imposing asymmetries on many scales in the circumstellar environment of this star.

References

- Baud, B., Habing, H. J., Matthews, H. E., & Winnberg, A., 1979, *A&A*, 35, 179
 Cotton, W. D., Jaffe, W.m, Perrin, G., & Woillez, J., 2008, *A&A*, 477, 517
 Goldreich Peter, Keeley, Douglas A., & Kwan, John Y., 1973, *ApJ*, 179, 111
 Herman, J. & Habing, H. J., 1985, *A&A*, 59, 523
 Kembell, A. J. & Diamond, P. J., 1997, *ApJ*, 481, 111
 Kembell, Athol J., Diamond, Philip J., Gonidakis, Ioannis, Mitra, Modhurita, Yim, Kijeong, Pan, Kuo-Chuan, & Chiang, Hsin-Fang, 2009, *ApJ*, 698, 1721
 Modjaz, Maryam, Moran, James M., Kondratko, Paul T., & Greenhill, Lincoln J., 2005, *ApJ*, 626, 104
 Nedoluha, Gerald E. & Watson, William D., 1990, *ApJ*, 361, 53
 Van Langevelde, H. J., van der Heiden, R., & van Schooneveld, C., 1990, *A&A*, 239, 193
 Watson, W. D., 2002, IAUS206, 206, 464
 Wiebe, D. S. & Watson, W. D., 1998, *ApJ*, 503, 71